



Research article

Quantity, distribution and phenotype of newly generated cells in the intact spinal cord of adult macaque monkeys

D. Marinova^{a,b}, M.N. Ivanov^{a,b}, T. Yamashima^c, A.B. Tonchev^{a,b,*}

^a Department of Anatomy and Cell Biology, Faculty of Medicine, Marin Drinov str. 55, Medical University, Varna, Bulgaria

^b Department of Stem Cell Biology, Research Institute, Medical University, Varna, Bulgaria

^c Department of Psychiatry and Behavioral Science, Kanazawa University Graduate School of Medical Sciences, Takara-machi 13-1, Kanazawa, Japan

ARTICLE INFO

Keywords:

Spinal cord
Proliferation
Central canal
Transcription factor

ABSTRACT

The existence of proliferating cells in the intact spinal cord, their distribution and phenotype, are well studied in rodents. A limited number of studies also address the proliferation after spinal cord injury, in non-human primates. However, a detailed description of the quantity, distribution and phenotype of proliferating cells at different anatomical levels of the intact adult non-human primate spinal cord is lacking at present. In the present study, we analyzed normal spinal cord tissues from adult macaque monkeys (*Macaca fuscata*), infused with Bromo-2'-deoxyuridine (BrdU), and euthanized at 2h, 2 weeks, 5 weeks and 10 weeks after BrdU. We found a significantly higher density of BrdU + cells in the gray matter of cervical segments as compared to thoracic or lumbar segments, and a significantly higher density of proliferating cells in the posterior as compared to the anterior horn of the gray matter. BrdU + cells exhibited phenotype of microglia or endothelial cells (~50%) or astroglial and oligodendroglial cells (~40%), including glial progenitor phenotypes marked by the transcription factors Sox9 and Sox10. BrdU + cells also co-expressed other transcription factors known for their involvement in embryonic development, including Emx2, Sox1, Sox2, Ngn1, Olig1, Olig2, Olig3. In the central canal, BrdU + cells were located along the dorso-ventral axis and co-labeled for the markers Vimentin and Nestin. These results reveal the extent of cellular plasticity in the spinal cord of non-human primates under normal conditions.

1. Introduction

The level of cell proliferation *in vivo* in the intact adult primate spinal cord is not well understood. *In vitro* evidence has indicated the presence of stem cells [1,2]. These cells are thought to be located in or adjacent to the ependymal layer of the central canal in the spinal cord [3–7]. In the normal adult spinal cord of the rat, Horner et al. (2000) [8] reported the presence of turnover of glial progenitors and mature glial cells, particularly in the white matter. In adult primate models, induction of spinal cord injury lead to massive glial proliferation [9] and even neurogenesis, in the posterior horn [10]. Another progenitor cell niche in the adult mammalian spinal cord is the central canal region, where ependymal cells seem the primary source of stem cells, they are rapidly activated after injury, and proliferate in the damaged tissue [11–13]. To the best of our knowledge, cell proliferation in the primate spinal cord under normal

* Corresponding author Department of Anatomy and Cell Biology, Faculty of Medicine, Marin Drinov str. 55, Medical University, Varna, Bulgaria.
E-mail address: anton.tonchev@mu-varna.bg (A.B. Tonchev).

<https://doi.org/10.1016/j.heliyon.2024.e28856>

Received 22 September 2023; Received in revised form 25 March 2024; Accepted 26 March 2024

Available online 29 March 2024

2405-8440/© 2024 Published by Elsevier Ltd.

This is an open access article under the CC BY-NC-ND license

(<http://creativecommons.org/licenses/by-nc-nd/4.0/>).

conditions has not been studied in detail.

In the present study we aimed to investigate the level of proliferation and the phenotype of newly generated cells throughout the intact spinal cord of adult macaque monkeys. We used a classical proliferation marker (bromodeoxyuridine; BrdU) to label newly generated cells and traced their quantity and phenotype at one short-term survival time point (2h), and three long-term survival points (2 weeks, 5 weeks and 10 weeks), after the BrdU infusion. We report the densities, distribution and phenotypes of the BrdU + cells using a panel of cell markers characteristic for different brain cells. In addition, we identified BrdU + cells expressing transcription factors that regulate the embryonic spinal cord development, which potentially constitute additional cellular subtypes undergoing cell division. Our data show the heterogeneity of the cellular populations undergoing plasticity in the adult monkey spinal cord under normal conditions.

2. Materials and methods

2.1. Experimental animals

The reported experimental procedures were performed following an approval by the Animal Care and Ethics Committee of Kanazawa University, Japan. We used tissues from 11 female adult Japanese monkeys (*Macaca fuscata*), aged 5–10 years. The monkeys were bred in air conditioned wide cages and were allowed free daily access to food and water.

2.2. BrdU paradigm

5-Bromo-2'-deoxyuridine (BrdU; Sigma-Aldrich) was dissolved in sterile saline with 0.007 N NaOH. Each monkey received 5 intravenous injections of 100 mg/kg BrdU (1 injection per day) into the saphenous vein, for 5 consecutive days [14,15]. The monkeys were sacrificed 2 h (n = 3), 2 weeks (n = 3), 5 weeks (n = 3) and 10weeks (n = 2) after the last BrdU injection (Fig. 1A).

2.3. Histology and immunostaining

The tissue processing was done according to a procedure published before [14,15]. Briefly, following a perfusion with 4% paraformaldehyde, the first 3 cervical (C1–C3), thoracic (Th1–Th3) and lumbar (L1–L3) spinal cord segments were extracted and postfixed. Following cryopreservation with sucrose, tissue blocks encompassing the thickness of one segment (C1, Th1, L1) were embedded into O.C.T. medium and the blocks were cut horizontally at 40 μ m. The sections were then stored in multi well plates at -25°C in cryopreservation buffer.

Free-floating sections were blocked and incubated in a solution containing the respective primary antibody for 36–48 h at 4°C [14, 15]. A list of primary antibodies is presented in Table 1. Following several washes, the sections were incubated with the secondary antibodies for 3–4 h at room temperature. Prior to BrdU immunostaining, DNA was denatured by formamide/standard sodium citrate buffer at 65°C for 2h followed by 2 N NaCl for 30 min at 37°C .

For single labeling by the immunoperoxidase method, the primary antibodies were visualized with the ABC Elite kit (Vector), followed by diaminobenzidine (DAB; Sigma) as a chromogen. For fluorescence double and triple labeling, the primary antibodies were visualized with antibodies conjugated to the following fluorochromes: Alexa Fluor-488, -546, -633 (ThermoFisher, USA), and TRITC (Jackson ImmunoResearch, USA). All secondary antibodies were applied for 2 h at room temperature. Finally the sections were mounted on glass slides and coverslipped under Entellan resin (Merck) for light or under Vectashield (Vector Labs, USA), for fluorescence microscopy.

2.4. Image acquisition and data analysis

Light microscopy of immunoperoxidase-stained sections was performed using an Olympus BX-60 microscope (Tokio, Japan). The spinal cord was divided into 6 regions of interest (Fig. 1B): 1) anterior horn of gray matter; 2) posterior horn of gray matter; 3) anterior

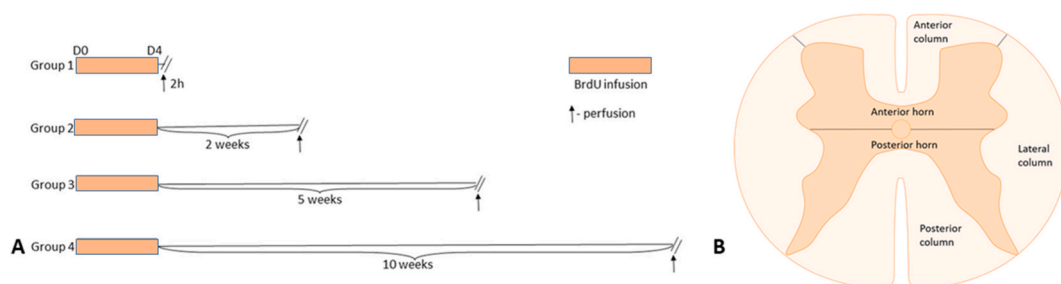


Fig. 1. Experimental paradigms. A. Time-frame of animal experiments and BrdU injection protocols used in the study. Group I is short term group; Groups II, III, IV could be combined in long term group. B. Schematic presentation of a horizontal section through the spinal cord. The regions of interest are annotated.

Table 1
Data for the primary antibodies used in the present study.

Antibodies	Species, isotype	Dilution	Marker for (reference)
Cell markers			
BrdU	mouse IgG	1:100	DNA synthesis [13,14]
	rat IgG	1:100	
Ki67	mouse IgG	1:50	Proliferating cells [15]
β -Tubulin, class III	mouse IgG	1:300	Neuronal progenitors [16,17]
	rabbit IgG	1:500	
A2B5	mouse IgG		[18]
NeuN	mouse IgG	1:100	Neurons [19]
GFAP	rabbit IgG	1:200	Astrocytes [20]
Iba 1	rabbit IgG	1:800	Microglia/Macrophages [21,22]
O4	mouse IgM	1:100	[23]
vWF	rabbit IgG	1:500	[24]
Nestin	Mouse IgM rabbit IgG	1:100	Neural progenitors, astrocytes [25]
		1:400	
Vimentin	Mouse IgG	1:100	Neural progenitors, astrocytes [26]
PSA-NCAM	Mouse IgG	1:100	Neuroblasts [27]
Transcription factors			
Emx 2	rabbit IgG	1:300	Early progenitors [28]
Ngn 1	rabbit IgG	1:1000	Neural progenitors [29]
Olig 1	rabbit IgG	1:1000	Oligodendrocyte precursors [29,30]
Olig 2	rabbit IgG	1:200	
Sox 1	rabbit IgG	1:200	Early progenitors/stem cells [31]
Sox 2	rabbit IgG	1:200	
Sox 9	rabbit IgG	1:150	[32,33]
Sox 10	rabbit IgG	Ready for use	[32–34]
Shh	rabbit IgG	1:50	[35]
Smo	rabbit IgG	1:50	[36]

column of white matter; 4) lateral column of white matter; 5) posterior column of white matter; 6) central canal region. The BrdU + cells and the area of each region of interest were evaluated on every 12th section through C1, Th1, and L1 segments in each monkey, and the BrdU + cells were quantified densitometrically (cells/mm²) for each section. The section densities within each region of interest were averaged for the C, Th, or L segments to obtain the density.

Double and triple labeling for BrdU and for various markers was verified using confocal laser scanning microscopy (LSM 700, Carl Zeiss). We performed Z sectioning at 0.5–1.0 μ m intervals and optical stags were used for analysis and for digital generation of three-dimensional reconstruction. Assembly and and brightness/contrast adjustments of all images were performed using Adobe Photoshop.

2.5. Statistics

Statistical analysis was performed using one-way ANOVA followed by Tukey-Kramer's post-hoc comparisons and two sided *t*-test. Data expressed the mean \pm SEM. Differences were considered significant when $p \leq 0.05$.

3. Results

3.1. Numerous de novo generated cells exist in the intact monkey spinal cord

Our first aim was to investigate for the presence, quantity and distribution of cells undergoing proliferation of the intact monkey spinal cord, at different anatomical levels (Figs. 2–3). We found on average \sim 250 BrdU + cells per section through the cervical, thoracic or lumbar segments. Of these, \sim 80 positive cells were located in the gray matter and \sim 170 cells were located in the white matter, per section. Since the areas of the gray and white matter differ at each segment, our statistical analyzes report densitometrical data (BrdU + cells/mm² within each region of interest at each segment).

We first calculated the density of BrdU + cells at a short survival time point following the BrdU infusion: 2 h after 5 consecutive BrdU injections (Group I, Fig. 1A), at different anatomical levels. We found a significantly higher density in the gray matter of both anterior (Fig. 2A–C) and posterior horns (Fig. 2D–F) at level C1 as compared to L1 or Th1. When we compared the density of proliferating cells in the anterior versus the posterior horns of the gray matter, we found a higher density in the posterior horn: 22 ± 5 BrdU + cells/mm² in the cervical posterior horn vs 17 ± 3 BrdU + cells in the cervical anterior horn, 19 ± 5 BrdU + cells in the thoracic posterior horn vs 10 ± 3 BrdU + cells in the thoracic anterior horn ($p < 0.01$, Tukey-Kramer test). There was no statistically significant difference between the anterior and posterior horn at lumbar levels. In the white matter, the density of BrdU + cells did not exhibit significant differences with respect to either anatomical level or column localization (anterior versus lateral or posterior columns) (Fig. 2G–O). The average BrdU + cell density in the gray matter (16 cells/mm²) was higher as compared to the white matter (11 cells/mm²).

About 10–12% of the BrdU + cells in both the gray and the white matter were located in “doublets” (Fig. 2A - inset) suggesting a

recent division. Morphologically, in both the gray and white matter, many BrdU + nuclei had an elongated (rod-shaped) appearance (Fig. 2G-inset), while a smaller fraction of the BrdU-labeled nuclei had a round shape (Fig. 2E-inset).

The distribution and morphological appearance of BrdU + cells were similar among three spinal levels examined (cervical, thoracic or lumbar).

3.2. Survival of newly generated cells in the spinal cord

To investigate whether the BrdU + cells observed immediately following BrdU infusion (monkeys of Group I; Fig. 1A) survive and what is their distribution in the intact spinal cord, we used tissues from experiments, in which the monkeys survived longer time points after BrdU (Fig. 1A): 2 weeks, 5 weeks, or 10 weeks. We observed a dramatic decrease of the BrdU + cells per section: from 250 BrdU + cells per section at 2h after BrdU to 80–100 positive cells per section at 2–10 weeks after BrdU (Fig. 3A–O). Statistical evaluation confirmed that the density of the BrdU + cells was significantly reduced beyond the 2h-time point (Fig. 4A). This decrease was evident in all studied spinal cord segments. We did not observe statistically significant differences among the three long-term survival groups: 2 weeks, 5 weeks or 10 weeks after BrdU (Fig. 4A). In addition to the reduction of the proliferating cell density in the animals surviving beyond the 2h-time point after BrdU, we also observed a reduction in the BrdU + cell doublets. In animals euthanized 2 weeks after BrdU, the fraction of BrdU + cells forming “doublets” was reduced to 5–6% of the BrdU + cells, while in the 10-week survival group the fraction of BrdU + cells forming “doublets” was below 1% (Fig. 4B).

To test the applicability of BrdU as a marker labeling dividing cells - Ki67 [18] at 2h after BrdU infusion. Double-staining between Ki67 and BrdU revealed that the majority (80%) BrdU + cells are also Ki67+ (Fig. 4C). In long term survival group, we found that 24% of all BrdU + cells are Ki67+.

3.3. Proliferation of endothelial and glial cells in the monkey spinal cord

We did not find BrdU signal in neuronal cells labeled by NeuN or other neuronal markers (data not shown).

We investigated whether BrdU is incorporated into cells with a phenotype of blood vessel endothelial cells, astrocytes, oligodendrocytes or glial progenitor cells (Table 1, Fig. 5F, 6F and 7).

Double-staining for BrdU and the microglial marker Iba1 (Ionized calcium binding adaptor molecule 1; [37]), demonstrated that many BrdU + cells were of a microglial phenotype (Figs. 5A and 6A). At the 2h survival time point after BrdU application, the BrdU+/Iba1+ cells comprised ~20% of all BrdU + cells (Fig. 7 A). With increased survival after BrdU, this fraction increased to nearly 40% of the BrdU% cells at 10 weeks after BrdU (Fig. 7 D). These data indicated that the microglial cell population represents a major dividing cell fraction in the primate spinal cord under normal conditions.

We used as marker of endothelial cells Von Willebrand factor (vWF) [27]. We found that at all survival time points after BrdU, the BrdU+/vWF + cells represented 20–30% of all BrdU + cells (Figs. 5E, 6E and 7A–D).

The marker A2B5 was used to investigate if there are BrdU + cells at the stage of bipotent glial progenitors (oligodendrocyte or astrocyte; [21]). We evaluated that the BrdU+/A2B5+ cells correspond to ~5% of BrdU + cells (Fig. 7A–D). Nearly all of them were

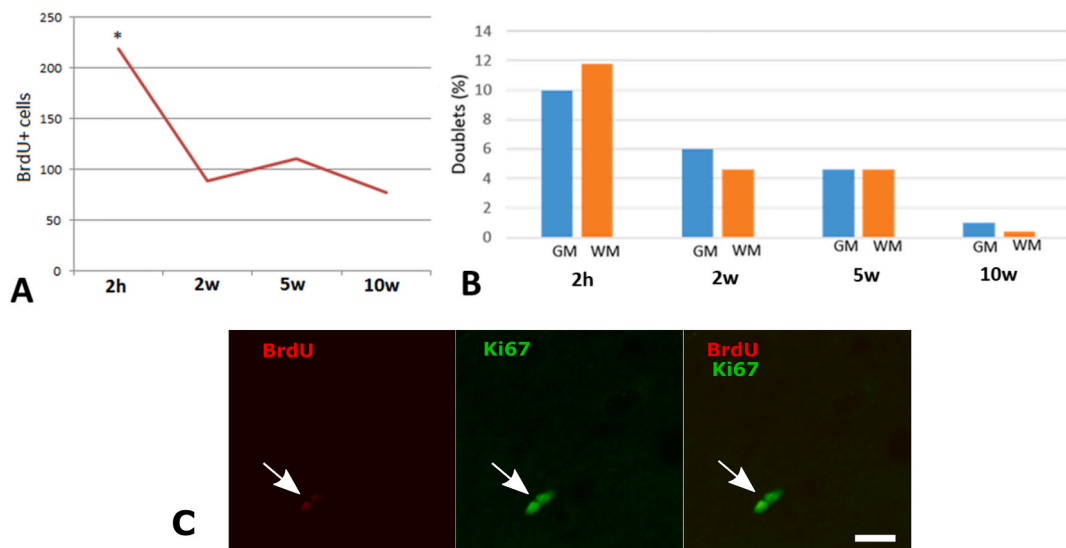


Fig. 4. Statistical evaluation of BrdU + cell density and BrdU + cell “doublets” at various time points after BrdU. A. Number of BrdU + cells per section. *, $P < 0.05$. B. Proportion of BrdU + cells located in “doublets” at 2h, 2 weeks (wk), 5 weeks or 10 weeks following the infusion with BrdU. C. Double-labeling for BrdU (red) and Ki67 (green) in gray matter of the spinal cord at 2h survival after BrdU. Scale bar, 40 μm.

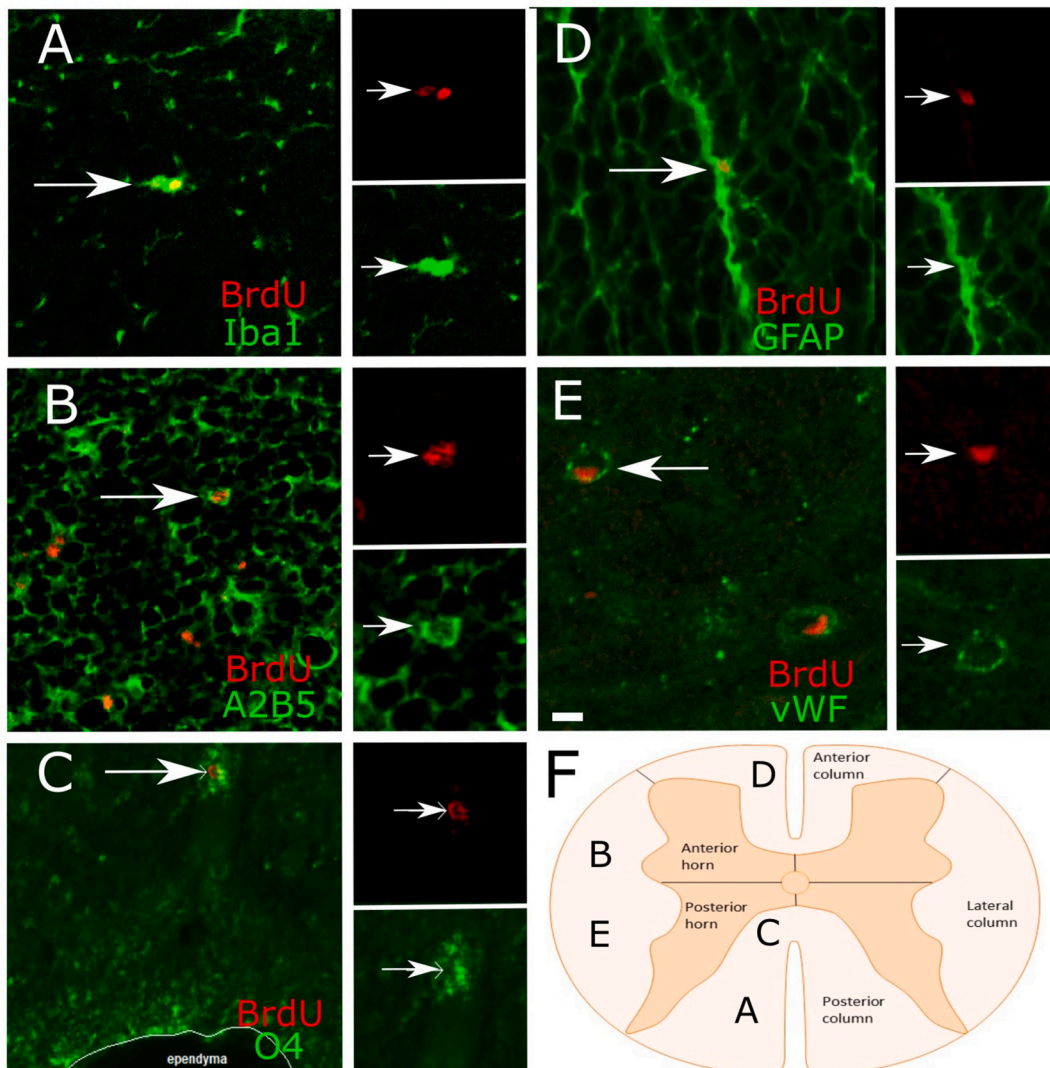


Fig. 5. Phenotype of BrdU + cells in the short-term survival group (2h after BrdU). A-E. Double-staining for BrdU (red) and different cell markers (green). Double-positive cells are depicted by arrows. F. Schematic map of the spinal cord indicating the position of the images from panels A-E. Scale bar, 10 μ m (E).

located in the white matter (Figs. 5B and 6B). The presence of BrdU-incorporating oligodendrocytes was probed by coming BrdU labeling with the marker O4, marker specific for the early-mid stages of oligodendrogenesis [26]. BrdU+/O4+ cells (Figs. 5C and 6C) represented 5% of the population of *de novo* generated cells (Fig. 7A–D) and were located in the white matter.

Astrocytic cells were visualized using antibody against the intermediate filament protein Glial Fibrillary Acidic Protein (GFAP). The percentage of proliferating astrocytes increased from less than 1% at 2h after BrdU (Fig. 5D and 7A) to about 7% at 10 weeks of survival after BrdU (Fig. 6D and 7D). We observed BrdU+/GFAP + cells in both the white and gray matter, but most of them were localized to in the white matter, associated with radial elements (Fig. 5D, arrow).

3.4. BrdU + cells express transcription factors involved in embryonic spinal cord development

We wanted to probe whether proliferating cells in the normal monkey spinal cord tissue express transcription factors known for their involvement in brain development, similarly to what shown in rodents [38]. Further, the phenotype of nearly 50% of BrdU + cells studied at the time point 2h after BrdU could not be classified with cell markers listed above (Fig. 7A), thus raising the possibility of the existence of undifferentiated cells which could potentially express such embryonic transcription factors. We therefore performed double-labeling for BrdU and transcription factors which are expressed in embryonic progenitors: Sox1, Sox2, Sox9, Sox10, Smo, Emx2, Ngn1, Olig1, Olig2, Olig3 [26,28,34–36,39–47].

Double-labeling for BrdU and Emx2 revealed that 9% (8 out of 86 cells) of the BrdU + cells were also Emx2+ (Fig. 8D).

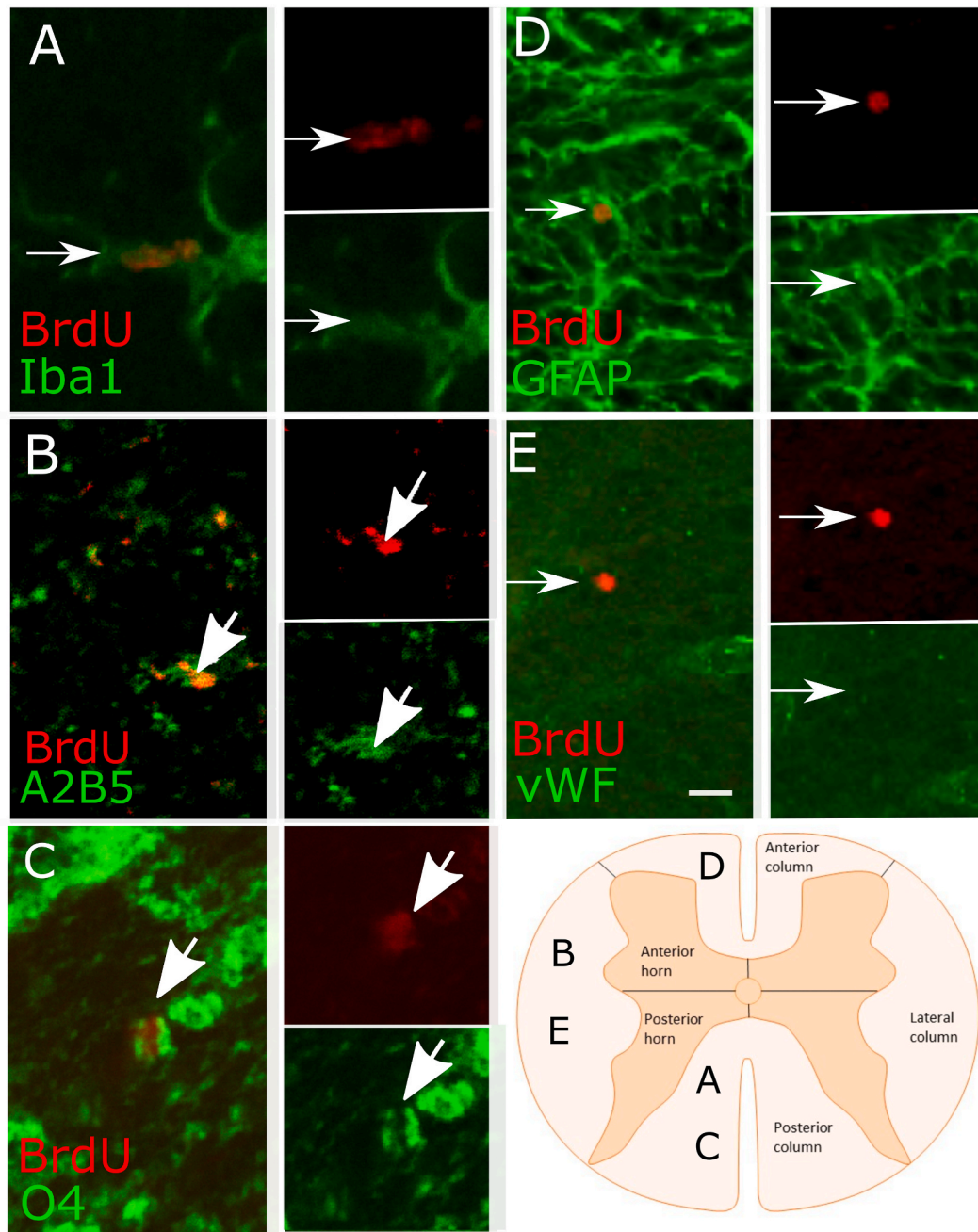


Fig. 6. Phenotype of BrdU + cells in a long-term survival group (5 weeks after BrdU). A-E. Double-staining for BrdU (red) and different cell markers (green). Double-positive cells are depicted by arrows. F. Schematic map of the spinal cord indicating the position of the images from panels A-E. Scale bar, 20 μm (E).

Combinations of BrdU labeling with stainings for transcription factors Sox1 or Sox2 revealed presence of dual-positive cells. Double-positive cells for BrdU/Sox1 were observed in the gray and white matter of the spinal cord (12%, 12 out of 100 BrdU + cells) (Fig. 8F), while BrdU/Sox2 cells (7%, 6 out of 93 BrdU + cells) were detected only in the white matter (Fig. 8G). A small fraction of BrdU + cells 4% (3 out of 95 cells) co-expressed the pro-neurogenic transcription factor Ngn1 (Fig. 8E).

Sox9 is expressed by both oligodendroglial and astroglial precursors, and subsequently remains expressed in the differentiation astroglial cells but not in the maturing and mature oligodendrocytes [32,33]. Our observations showed that Sox9 was expressed by the cells which are located only within the borders of the gray matter of the spinal cord. They are also seen around the central canal, but not in the ependymal layer and subependymal zone. Some of the described cells were located in doublets. In the short term survival

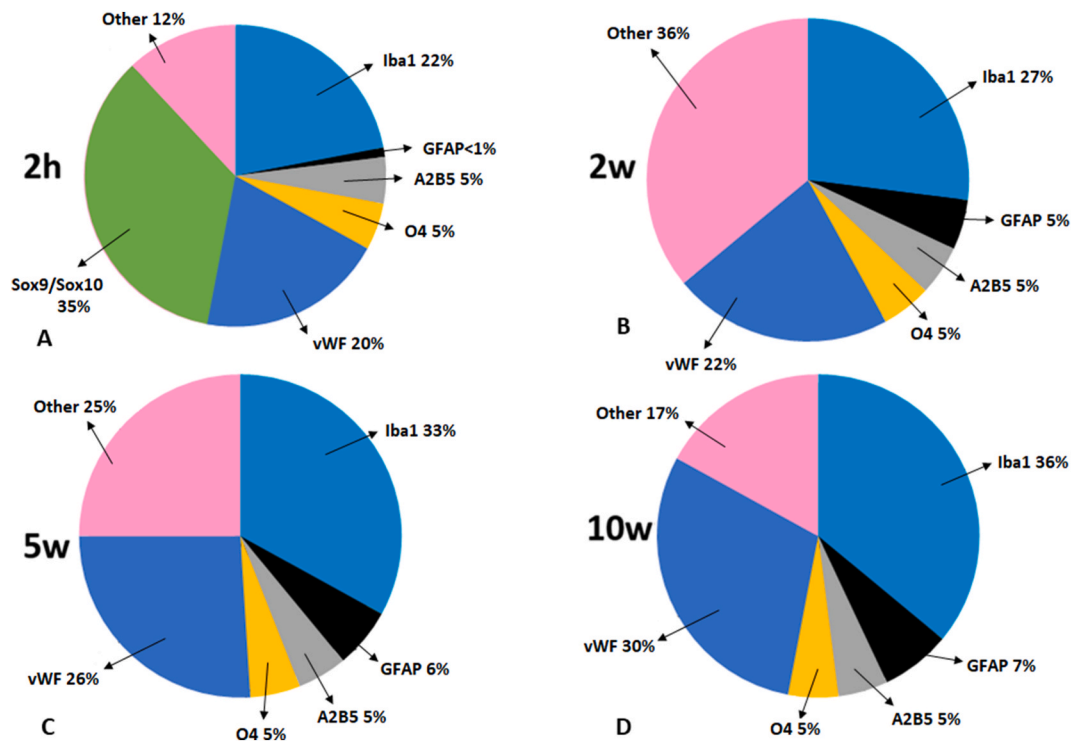


Fig. 7. Proportions of proliferating cells expressing cell specific markers at different survival time points after BrdU: A- 2 h (2h), B, C, D- 2–10 weeks (2w/5w/10w).

animals we observed that 28% of the BrdU + cells co-expressed Sox9 (27 out of 96 cells) (Fig. 8H).

Sox10 is a transcription factor that marks all developmental phases of oligodendrocytogenesis [32–34]. In the macaque spinal cord, BrdU+/Sox10+ were predominantly observed within the gray matter with just a few double-stained cells in the white matter. At short term survival after BrdU, we observed 35% double-labeled cells (34 out of 103 BrdU + cells) (Fig. 8I).

Co-staining BrdU with the oligodendrocyte transcription factors Olig1, Olig2, Olig3, we found that BrdU+/Olig1+ cells as well as BrdU+/Olig2+ cells were detected only in white matter of short term group (3%, 3 out of 98 BrdU + cells), but BrdU+/Olig3+ cells were found in both white and gray matter of the spinal cord (7%, 8 out of 94 cells) in monkeys from the same survival group (Fig. 8A,B, C).

By double labeling with Smo, the transmembrane receptor of the morphogen Sonic hedgehog (Shh) [48], we found a small number (3%, 3 of 97 BrdU + cells) of BrdU+/Smo + cells localized in the white matter of the short term group (Fig. 8J).

3.5. Distribution and phenotype of proliferating cells in the central canal

Immunostaining for BrdU revealed positive cells in the central canal region, typically immediately beneath to the ependymal layer, in both short-term and long-term survival animals after BrdU (Fig. 9A and B; arrows). Most of the BrdU + cells were situated at the ventral or the dorsal poles of the central canal. BrdU + cells were also observed within the ependymal layer (inset in Fig. 9A and B). Similarly to the gray and white matter, the BrdU + cells in the central canal region decreased with the prolonged time interval following the BrdU infusion (Fig. 9C).

Labeling for Vimentin revealed a strong signal in the central canal, which was topographically organized along the dorso-ventral axis, with strongly labeled cells at the ventral pole (toward the anterior fissure) and the dorsal pole (toward the posterior fissure) of the canal (Fig. 9E1, arrows; see the map in panel D). Many ependymal cells expressed Vimentin in their cytoplasm, but the cells at the poles projected processes along the dorso-ventral axis (Fig. 9E3, arrowheads). We detected Vimentin+/BrdU + cells which were located immediately beneath the ependymal layer (Fig. 9E2-E3, arrow) or within a few hundred μm away from the ependymal layer of the central canal, at the dorsal side of the canal (Fig. 9E4-E5, arrow). However, we did not observe a subependymal layer of cells, anatomically separate from the ependymal layer as seen in the subventricular zone of the lateral ventricle.

Immunostaining for PSA-NCAM showed cytoplasmic signal in most ependymal cells of the canal (Fig. 9F1) with the cells at the dorsal of the canal showing the highest signal intensity (Fig. 9F1-F2, arrows). At the dorsal pole, PSA-NCAM + cells seemed like forming a chain extending in the posterior direction (Fig. 9F2, arrows). Unlike for PSA-NCAM, the ependymal layer of the canal was negative for GFAP, but a dense meshwork of GFAP + processes surrounded the ependymal cells (Fig. 9G, arrows). Numerous blood vessels, revealed by vWF immunostaining were visible in close vicinity to the central canal, but did not come into a direct contact with

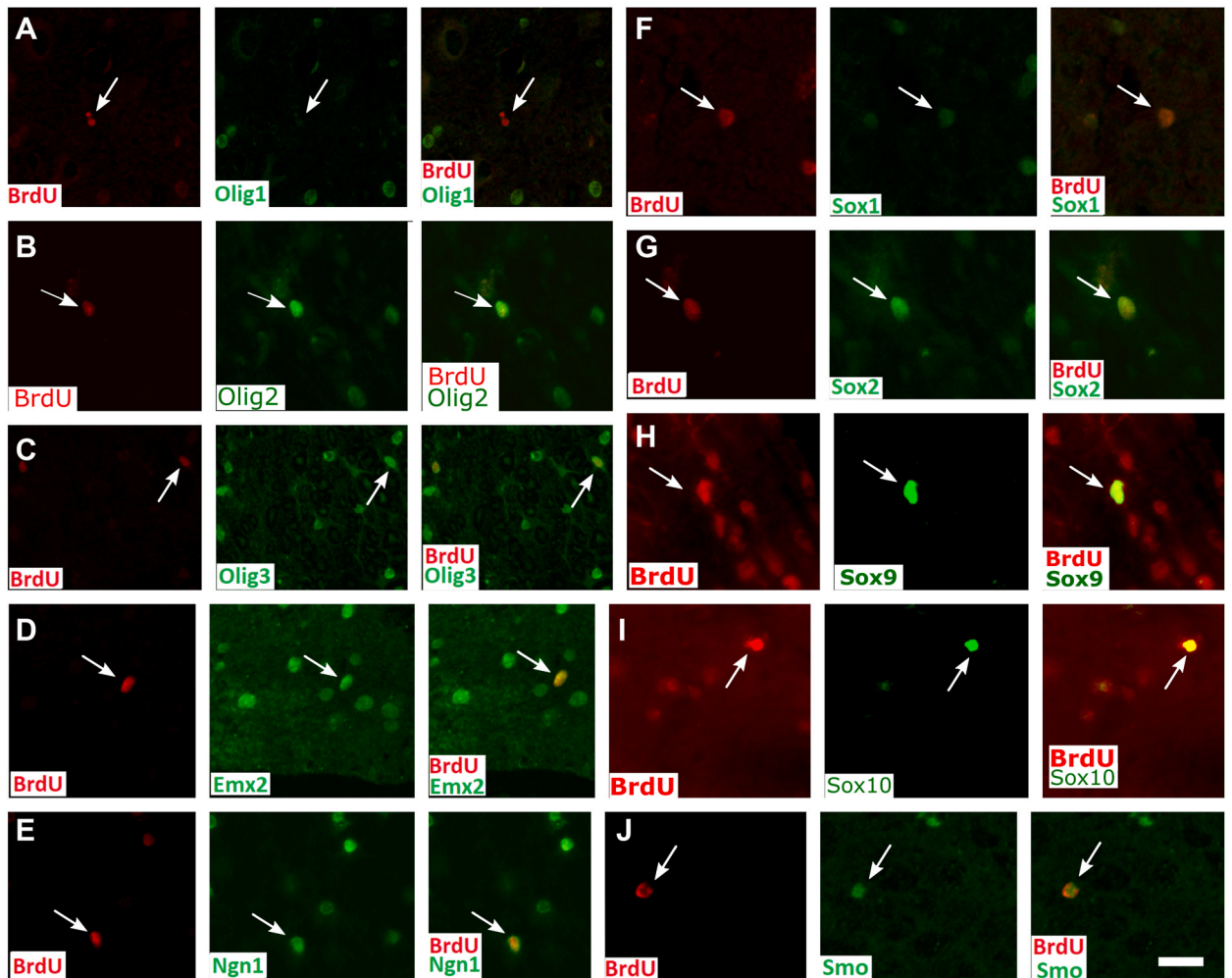


Fig. 8. Proliferating cells express embryonic transcription factors in adult monkey spinal cord. Double-staining for BrdU (red) and different transcriptions (green) in the spinal cord of the short-term survival group (2h after BrdU). Double-positive cells are depicted by arrows. Scale bar, 20 μ m (H).

the ependymal cells (Fig. 9H, arrows). Of note, some of the processes of the Vimentin + cells originating from the central canal reached to blood vessels (Fig. 9I2, arrow).

Similarly to PSA-NCAM, the marker Nestin labeled cells at both the dorsal and ventral poles of the canal, with a stronger staining at the dorsal pole (Fig. 9I1, arrowhead). Double-labeling for Vimentin and Nestin showed the presence of dual positive cells (Fig. 9I1–I3, arrowheads).

4. Discussion

The present study provides the first detailed data on the amount and phenotype of proliferating cells in the intact spinal cord of adult primates.

4.1. Cellular proliferation in monkey spinal cord differs across the dorso-ventral and the rostro-caudal axes

The present study provides comprehensive data on cell proliferation in the intact spinal cord of adult macaque monkeys. Cell proliferation was studied across two axes: (i) dorso-ventral axis (anterior versus posterior horn of the gray matter; anterior versus lateral versus posterior column of the white matter), and (ii) rostro-caudal axis (cervical versus thoracic versus lumbar spinal cord levels). Our data indicate a higher level of proliferation in the dorsal gray matter of the monkey spinal cord as compared to ventral horn. Further, we detected higher proliferation at more rostral (cervical) levels as compared to more caudal (thoracic or cervical) levels. Data in normal rat spinal cord [8] demonstrate higher quantity of BrdU + cells in the outer circumference of the spinal cord, while in the monkey we found greater BrdU + cell density in the gray matter as compared to the white matter. Of note, cellular

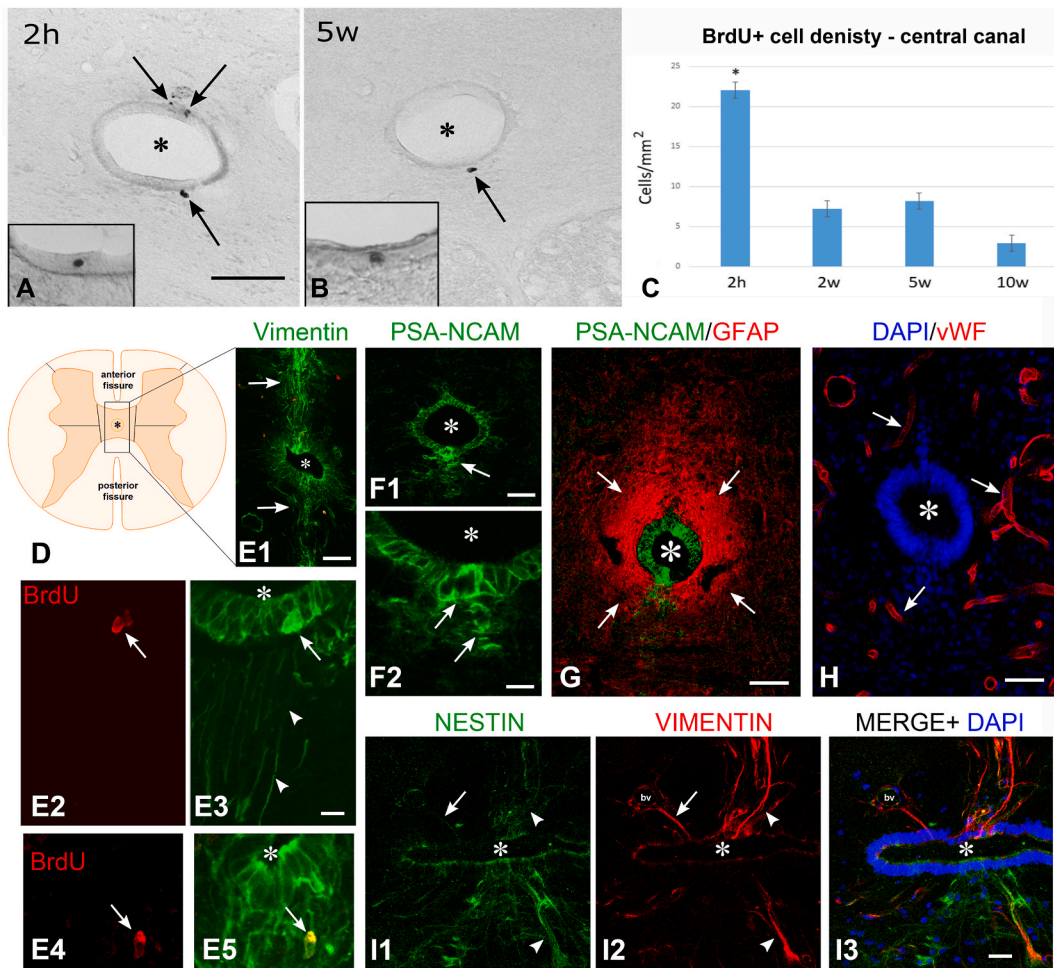


Fig. 9. Location and phenotype of BrdU + cells in the central canal of the macaque spinal cord. A-C. BrdU immunolabeling of monkey sections at 2h (A) and 5 weeks (B) following BrdU infusion. The BrdU + cells are at the ventral or the dorsal poles of the canal (arrows). The images are aligned according the map in panel D. Insets demonstrate BrdU + cells within the ependymal layer. C. Statistical evaluation of the BrdU + cell density in the central canal after different survival times following BrdU application. *, $P < 0.05$. E. Immunostaining for Vimentin (green) and BrdU (red) demonstrates the dorso-ventral arrangement of the Vimentin + cells (E1; arrows). Double-labeled cells in E2-E5 are depicted by arrows. In panel E5, Vimentin + basal processes are depicted by arrowheads. F. Immunostaining for PSA-NCAM demonstrates numerous positive cells in the ependymal layer of the canal with the strongest signal at the dorsal pole (arrows). G. Dual immunolabeling for PSA-NCAM (green) and GFAP (red) demonstrates the lack of GFAP staining in the ependymal cells and a dense meshwork of fibers surrounding the canal (arrows). H. Anti-vWF (red) immunolabeling counterstained by DAPI shows the anatomical relation of blood vessels (arrows) to the central canal. I. Nestin/Vimentin double-staining revealing double-positive cells at the ventral and dorsal poles of the central canal (arrows). A basal process directed toward a blood vessel (bv) is depicted by an arrowhead. Asterisk, lumen of the central canal. Scale bars, 50 μm (A, B, E1, F1, G, H); 20 μm (F2, I3); 10 μm (E3).

plasticity was reportedly higher in the posterior horn of monkey spinal cord after injury [10]. This difference opens the possibility of differential topography of progenitor cell location or capacity across different axes, similarly to the forebrain subventricular zone [49].

4.2. Cellular proliferation in monkey spinal cord is sustained even in the absence of injury

Our data showed a reduction of the proliferating cells over time (Fig. 4A). However, the density of BrdU + cells was sustained when we compared the time points of 2 weeks, 5 weeks and 10 weeks after BrdU. These data indicate that some of the proliferating cells are short-lived, but a significant fraction sustains their existence over time. Of note, in normal rat spinal cord, quantity of proliferating cells was not dramatically induced at 4 weeks after BrdU as compared to 1 day after BrdU [8]. This might indicate mechanisms which eliminate around half of the newly formed cells in primates within a few days after birth. Another possible explanation of these findings could be that continued cell proliferation could lead to loss of the BrdU signal over time. Further studies are needed to address this phenomenon.

4.3. Microglial cells are a major proliferating cell fraction in primate spinal cord

An interesting finding of our study is the in primates microglial cells represent a large proliferating cell fraction. Proliferating microglial cells were detected in both anterior and posterior horns of the gray matter as well as in the white matter. Of note the fraction of BrdU + microglial cells was not reduced over time and it was even increased in the tissues with BrdU incorporation of 10 weeks time, suggesting a stable proliferation rate of microglial cells over time. Microglial cells respond to injury and their proliferation was markedly enhanced by spinal cord trauma [9]. In comparison to primate, in normal rat spinal cord proliferating microglial or endothelial cells were less than 5% [8]. What is the function of proliferating spinal cord microglia under normal conditions remains to be elucidated.

Macroglial cells represented another proliferating cell fraction of a significant size in monkey spinal cord. While BrdU + cells expressing the oligodendroglial (A2B5 or O4) or astroglial (GFAP) markers were around 10%, the co-labeling of BrdU with the transcription factors Sox9 and Sox10 revealed that about a third of the proliferating cells co-expressed these proteins. Sox9 is initially expressed by bipotent glial (oligodendroglial or astroglial) precursors, but at maturation of the cells labels preferentially astroglial cells [32,33], while Sox10 is a selective oligodendroglial marker [32–34]. These results suggest that in the intact primate spinal cord microglial and macroglial cells represent similar in size proliferating cell fractions. This is different to what is known for the intact rodent spinal cord [8] where microglial cells constitute a significantly larger proliferating cell fraction as compared to the macroglial cells.

The lack of neurogenesis in monkey spinal cord is in agreement with the results in rodents [8], where a larger number of BrdU + cells are present in the *Zona gelatinosa* of the posterior horns of the gray matter, but also no signs of neuronal proliferation are found under normal conditions.

4.4. Newly generated cells in monkey spinal cord express embryonic transcription factors

Newly generated cells in the normal rat spinal cord express transcription factors involved in embryonic spinal cord development [50]. We tested whether proliferating cells primate spinal cord would show similar expression. Indeed, transcription factors such as the Olig proteins Olig1, Olig2, Olig3 were expressed in the monkey and showed differential distribution: while BrdU+/Olig1+ and BrdU+/Olig2+ cells were found only in the white matter, BrdU+/Olig3+ cells were observed in both the gray and white matter. This indicates a heterogeneity of potential glial progenitors in the primate spinal cord [32].

Notably, two transcription factors known for their role in telencephalic neurogenesis were expressed by BrdU + cells in monkey spinal cord: Emx2 [51], and Ngn1, while expression of Ngn2 was not detected. Ngn1 and Ngn2 play a role in the regulation of dorsal plate progenitors during embryonic development of the spinal cord [52,53]. Lack of pro-neuronal transcription factor expression by proliferating cells in the monkey might contribute to the presence of unfavorable environment for progenitors [50] in the primate.

4.5. The central canal of the intact monkey spinal cord as a putative progenitor cell niche

We detected proliferating cells within the ependymal layer of the central canal, immediately beneath it, or in its vicinity (within a few hundred μm of the canal's lumen). Most of the BrdU + cells were topographically located at either the ventral or the dorsal poles of the canal. This dorso-ventral distribution of proliferating cells resembled the dorso-ventral arrangement of the cells, positive for Vimentin, Nestin or PSA-NCAM. Consequently, we observed that BrdU + cells typically co-labeled with Vimentin. Similar results with numerous BrdU+/Vimentin + cells in the central canal have been reported in rodents [12] named radial ependymal cells. However, in the rodent these cells are typically localized on the lateral side of the central canal [12], while in the monkey they were located at the dorsal pole. Further, in the monkey we also detected BrdU+/Vimentin + cells in subependymal position. The Vimentin + radial processes co-labeled for Nestin in the monkey, but not for GFAP, discordant with the reported in rodents GFAP co-expression of Vimentin + cells [54]. Unlike the expression pattern of GFAP, the pattern of Nestin expression in the central canal of rodent [13,55] and primate (this study) was similar, with stronger Nestin expression at the dorsal pole and weaker expression at the ventral pole.

The strong expression of Vimentin, Nestin and PSA-NCAM at the dorsal pole, and the predominantly dorsal localization of BrdU+/Vimentin + cells in the monkey central canal suggest that this domain of the central canal is a putative progenitor cell niche in the primate.

Funding

This work was supported by the European Commission Horizon 2020 Framework Programme (Project 856871 — TRANSTEM), and Kiban-Kennkyu (B) (19H04029) from the Japanese Ministry of Education, Culture, Sports, Science and Technology (T.Y.).

CRediT authorship contribution statement

D. Marinova: Writing – original draft, Visualization, Methodology, Formal analysis, Data curation. **M.N. Ivanov:** Investigation. **T. Yamashima:** Writing – review & editing, Resources, Funding acquisition, Conceptualization. **A.B. Tonchev:** Writing – original draft, Resources, Project administration, Investigation, Funding acquisition, Formal analysis, Conceptualization.

Declaration of competing interest

The authors declare the following financial interests/personal relationships which may be considered as potential competing interests:

Anton Tonchev reports financial support was provided by Medical University Varna Prof Dr Paraskev Stoyanov. Tetsumori Yamashima reports financial support was provided by Kanazawa University Graduate School of Medical Sciences.

References

- [1] S. Weiss, C. Dunne, J. Hewson, C. Wohl, M. Wheatley, A.C. Peterson, B.A. Reynolds, Multipotent CNS stem cells are present in the adult mammalian spinal cord, *J. Neurosci.* 16 (1996) 7599–7609, <https://doi.org/10.1523/JNEUROSCI.16-23-07599.1996>.
- [2] L.S. Shihabuddin, J. Ray, F.H. Gage, FGF-2 is sufficient to isolate progenitors found in the adult mammalian spinal cord, *Exp. Neurol.* 148 (1997) 577–586, <https://doi.org/10.1006/exnr.1997.6697>.
- [3] C.M. Morshead, B.A. Reynolds, C.G. Craig, M.W. McBurney, W.A. Staines, D. Morassutti, S. Weiss, D. van der Kooy, Neural stem cells in the adult mammalian forebrain: a relatively quiescent subpopulation of subependymal cells, *Neuron* 13 (1994) 1071–1082, [https://doi.org/10.1016/0896-6273\(94\)90046-9](https://doi.org/10.1016/0896-6273(94)90046-9).
- [4] J.M. Garcia-Verdugo, F. Doetsch, H. Wichterle, D.A. Lim, A. Alvarez-Buylla, Architecture and cell types of the adult subventricular zone: in search of the stem cells, *J. Neurobiol.* 36 (1998) 234–248, [https://doi.org/10.1002/\(sici\)1097-4695\(199808\)36:2<234::aid-neu10>3.0.co;2-e](https://doi.org/10.1002/(sici)1097-4695(199808)36:2<234::aid-neu10>3.0.co;2-e).
- [5] B.J. Chiasson, V. Tropepe, C.M. Morshead, D. van der Kooy, Adult mammalian forebrain ependymal and subependymal cells demonstrate proliferative potential, but only subependymal cells have neural stem cell characteristics, *J. Neurosci.* 19 (1999) 4462–4471, <https://doi.org/10.1523/JNEUROSCI.19-11-04462.1999>.
- [6] F. Doetsch, I. Caille, D.A. Lim, J.M. Garcia-Verdugo, Subventricular zone astrocytes are neural stem cells in the adult mammalian brain, *Cell* 97 (1999) 703–716, [https://doi.org/10.1016/s0092-8674\(00\)80783-7](https://doi.org/10.1016/s0092-8674(00)80783-7).
- [7] C.B. Johansson, S. Momma, D.L. Clarke, M. Risling, U. Lendahl, J. Frisen, Identification of a neural stem cell in the adult mammalian central nervous system, *Cell* 96 (1999) 25–34, [https://doi.org/10.1016/s0092-8674\(00\)80956-3](https://doi.org/10.1016/s0092-8674(00)80956-3).
- [8] P.J. Horner, A. Power, G. Kempermann, H.G. Kuhn, T.D. Plamer, J. Winkler, L. Thal, F. Gage, Proliferation and differentiation of progenitor cells through the intact adult rat spinal cord, *J. Neurosci.* 20 (6) (2000) 2218–2228, <https://doi.org/10.1523/JNEUROSCI.20-06-02218.2000>.
- [9] H. Yang, P. Lu, H. McKay, T. Bernot, H. Keirstead, O. Steward, F. Gage, V. Edgerton, M. Tuszynski, Endogenous neurogenesis replaces oligodendrocytes and astrocytes after primate spinal cord injury, *J. Neurosci.* 26 (2006) 2157–2166, <https://doi.org/10.1523/JNEUROSCI.4070-05.2005>.
- [10] M. Vessal, A. Aycok, M.T. Garton, M. Ciferri, C. Darian-Smith, Adult neurogenesis in primate and rodent spinal cord: comparing a cervical dorsal rhizotomy with a dorsal column transection, *Eur. J. Neurosci.* 26 (10) (2007) 2777–2794, <https://doi.org/10.1111/j.1460-9568.2007.05871.x>.
- [11] J.-P. Hugnot, The spinal cord neural stem cell niche, in: T. Sun (Ed.), *Neural Stem Cells and Therapy*, InTech, 2012, <https://doi.org/10.5772/30868>.
- [12] K. Meletis, F. Barnabé-Heider, M. Carlén, E. Evergren, N. Tomilin, O. Shupliakov, J. Frisen, Spinal cord injury reveals multilineage differentiation of ependymal cells, *PLoS Biol.* 6 (2008) e182, <https://doi.org/10.1371/journal.pbio.0060182>.
- [13] L. Hamilton, M. Truong, M. Bednarczyk, A. Aumont, K.J. Fernandes, Cellular organization of the central canal ependymal zone, a niche of latent neural stem cells in the adult mammalian spinal cord, *Neuroscience* 164 (2009) 1044–1056, <https://doi.org/10.1016/j.neuroscience.2009.09.006>.
- [14] A.B. Tonchev, T. Yamashima, L. Zhao, H. Okano, Differential proliferative response in the postschismic hippocampus, temporal cortex, and olfactory bulb of young adult macaque monkeys, *Glia* 42 (2003) 209–224, <https://doi.org/10.1002/glia.10209>.
- [15] A.B. Tonchev, T. Yamashima, K. Sawamoto, H. Okano, Transcription factor protein expression patterns by neural or neuronal progenitor cells of adult monkey subventricular zone, *Neuroscience* 139 (2006) 1355–1367, <https://doi.org/10.1016/j.neuroscience.2006.01.053>.
- [16] D.S. Packard, R.A. Menzies, D.G. Skalko, Incorporation of thymidine and its analogue, bromodeoxyuridine, into the embryos and maternal tissues of the mouse, *Differentiation* 1 (1973) 397–405, <https://doi.org/10.1111/j.1432-0436.1973.tb00137.x>.
- [17] M.W. Miller, R.S. Nowakowski, Use of bromodeoxyuridine-immunohistochemistry to examine the proliferation, migration and time of origin of cells in the central nervous system, *Brain Res.* 457 (1988) 44–52, [https://doi.org/10.1016/0006-8993\(88\)90055-8](https://doi.org/10.1016/0006-8993(88)90055-8).
- [18] T. Scholzen, J. Gerdes, The Ki-67 protein: from the known and the unknown, *J. Cell. Physiol.* 182 (2000) 311–322, [https://doi.org/10.1002/\(SICI\)1097-4652\(200003\)182:3<311::AID-JCP1>3.0.CO;2-9](https://doi.org/10.1002/(SICI)1097-4652(200003)182:3<311::AID-JCP1>3.0.CO;2-9).
- [19] M.K. Lee, L.I. Rebhun, A. Frankfurter, Posttranslational modification of class III beta-tubulin, *Proc. Natl. Acad. Sci. U.S.A.* 87 (1990) 7195–7199, <https://doi.org/10.1073/pnas.87.18.7195>.
- [20] V. Pancea, K.D. Bingaman, S.J. Wiegand, M.B. Luskin, Infusion of brain-derived neurotrophic factor into the lateral ventricle of the adult rat leads to new neurons in the parenchyma of the striatum, septum, thalamus, and hypothalamus, *J. Neurosci.* 21 (2001) 6706–6717, <https://doi.org/10.1523/JNEUROSCI.21-17-06706.2001>.
- [21] F. Blakemore, J. Franklin, J. Grang, Repair of demyelinated lesions by glial cell transplantation, *J. Neurol.* 242 (1994) S61–S63, <https://doi.org/10.1007/BF00939245>.
- [22] R. Mullen, C. Buck, A. Smith, NeuN, a neuronal specific nuclear protein in vertebrates, *Development* 116 (1992) 201–211, <https://doi.org/10.1242/dev.116.1.201>.
- [23] B.E. Boyes, S.U. Kim, V. Lee, S.C. Sung, Immunohistochemical co-localization of S-100b and the glial fibrillary acidic protein in rat brain, *Neuroscience* 17 (1986) 857–865, [https://doi.org/10.1016/0306-4522\(86\)90050-3](https://doi.org/10.1016/0306-4522(86)90050-3).
- [24] Y. Imai, I. Ibata, D. Ito, K. Ohsawa, S. Kohsaka, A novel gene *iba1* in the major histocompatibility complex class III region encoding an EF hand protein expressed in a monocytic lineage, *Biochem. Biophys. Res. Commun.* 224 (1996) 855–862, <https://doi.org/10.1006/bbrc.1996.1112>.
- [25] D. Ito, Y. Imai, K. Ohsawa, K. Nakajima, Y. Fukuchi, S. Kohsaka, Microglia-specific localization of a novel calcium binding protein, *Iba1*, *Brain Res Mol Brain Res* 57 (1998) 1–9, [https://doi.org/10.1016/s0169-328x\(98\)00040-0](https://doi.org/10.1016/s0169-328x(98)00040-0).
- [26] F. Pistollato, H.L. Chen, P.H. Schwartz, G. Basso, D.M. Panchision, Oxygen tension controls the expansion of human CNS precursors and the generation of astrocytes and oligodendrocytes, *Mol. Cell. Neurosci.* 35 (2007) 424–435, <https://doi.org/10.1016/j.mcn.2007.04.003>.
- [27] S. Park, O.M. Tepper, R.D. Galiano, J.M. Capla, S. Baharestani, M.E. Kleinman, Selective recruitment of endothelial progenitor cells to ischemic tissues with increased neovascularization, *Plast. Reconstr. Surg.* 113 (2004) 284–293, <https://doi.org/10.1097/01.PRS.0000091169.51035.A5>.
- [28] N. Duggal, R. Schmidt-Kastner, A.M. Hakim, Nestin expression in reactive astrocytes following focal cerebral ischemia in rats, *Brain Res.* 768 (1997) 1–9, [https://doi.org/10.1016/s0006-8993\(97\)00588-x](https://doi.org/10.1016/s0006-8993(97)00588-x).
- [29] N. Heins, F. Cremsi, P. Malatesta, R.M. Gangemi, G. Corte, J. Price, G. Goudreau, P. Gruss, M. Gotz, *Emx2* promotes symmetric cell divisions and a multipotential fate in precursors from the cerebral cortex, *Mol. Cell. Neurosci.* 18 (2001) 485–502, <https://doi.org/10.1006/mcne.2001.1046>.
- [30] G. Alonso, Neuronal progenitor-like cells expressing polysialylated neural cell adhesion molecule are present on the ventricular surface of the adult rat brain and spinal cord, *J. Comp. Neurol.* 414 (1999) 149–166, [https://doi.org/10.1002/\(sici\)1096-9861\(19991115\)414:2<149::aid-cne2>3.0.co;2-o](https://doi.org/10.1002/(sici)1096-9861(19991115)414:2<149::aid-cne2>3.0.co;2-o).
- [31] C. Schuurmans, O. Armant, M. Nieto, J.M. Stenman, O. Britz, N. Klenin, C. Brown, L.M. Langevin, J. Seibt, H. Tang, J.M. Cunningham, R. Dyck, C. Walsh, K. Campbell, F. Polleux, F. Guillemot, Sequential phases of cortical specification involve Neurogenin-dependent and -independent pathways, *EMBO J.* 23 (2004) 2892–2902, <https://doi.org/10.1038/sj.emboj.7600278>.
- [32] D.H. Rowitch, Glial specification in the vertebrate neural tube, *Nat. Rev. Neurosci.* 5 (2004) 409–419, <https://doi.org/10.1038/nrn1389>.
- [33] M. Bylund, E. Andersson, B.G. Novitsch, J. Muhr, Vertebrate neurogenesis is counteracted by Sox1-3 activity, *Nat. Neurosci.* 6 (2003) 1162–1168, <https://doi.org/10.1038/nn1131>.

- [34] R. Florian, M. Stephan, J. Waldeck, V. Huber, D. Demetriou, N. Kannaiyan, S. Galinski, L. Glaser, M. Wehr, M. Ziller, A. Schmitt, P. Falkai, M. Rossner, Expression of lineage transcription factors identifies differences in transition states of induced human oligodendrocyte differentiation, *Cells* 11 (2022) 241, <https://doi.org/10.3390/cells11020241>.
- [35] H. Huang, W. He, T. Tang, M. Qiu, Immunological markers for central nervous system glia, *Neurosci. Bull.* 39 (3) (2023) 379–392, <https://doi.org/10.1007/s12264-022-00938-2>.
- [36] a-Leo'n J. Garcí, M. Kumar, R. Boon, D. Chau, J. One, E. Wolfs, K. Eggermont, P. Berckmans, N. Gunhanlar, F. Vrij, B. Lendemeijer, B. Pavie, N. Corthout, S. Kushner, J. Da'vila, I. Lambrechts, W. Hu, C. Verfaillie, SOX10 single transcription factor-based fast and efficient generation of oligodendrocytes from human pluripotent stem cells, *Stem Cell Rep.* 10 (2018) 655–672, <https://doi.org/10.1016/j.stemcr.2017.12.014>.
- [37] Y. Imai, S. Kohsaka, H. Kanazawa, K. Ohsawa, Y. Sasaki, Macrophage/microglia-specific protein Iba1 enhances membrane ruffling and Rac activation via phospholipase C-gamma -dependent pathway, *Biol. Chem.* 277 (22) (2002) 20026–20032, <https://doi.org/10.1074/jbc.M109218200>.
- [38] R. Machold, R. Hayashi, M. Rutlin, M.D. Muzumadar, S. Nery, J.G. Corbin, A. Gritlin-Lunde, T. Dellovade, J.A. Porter, L.L. Rubin, H. Dudek, A.P. McMachon, G. Fishel, Sonic hedgehog is required for progenitor cell maintenance in telencephalic stem cell niches, *Neuron* 39 (2003) 937–950, [https://doi.org/10.1016/s0896-6273\(03\)00561-0](https://doi.org/10.1016/s0896-6273(03)00561-0).
- [39] S.P. Fancy, C. Zhao, R.J. Franklin, Increased expression of Nkx2.2 and Olig2 identifies reactive oligodendrocyte progenitor cells responding to demyelination in the adult CNS, *Mol. Cell. Neurosci.* 27 (2004) 247–254, <https://doi.org/10.1016/j.mcn.2004.06.015>.
- [40] H. Fu, Y. Qi, M. Tan, J. Cai, H. Takebayashi, M. Nakafuku, W. Richardson, M. Qiu, Dual origin of spinal oligodendrocyte progenitors and evidence for the cooperative role of Olig2 and Nkx2.2 in the control of oligodendrocyte differentiation, *Development* 129 (2002) 681–693, <https://doi.org/10.1242/dev.129.3.681>.
- [41] R. Galli, R. Fiocco, L. De Filippis, L. Muzio, A. Gritti, S. Mercurio, V. Broccoli, M. Pellegrini, A. Mallamaci, A.L. Vescovi, Emx2 regulates the proliferation of stem cells of the adult mammalian central nervous system, *Development* 129 (2002) 1633–1644, <https://doi.org/10.1242/dev.129.7.1633>.
- [42] Q.R. Lu, D. Yuk, J.A. Alberta, Z. Zhu, I. Pawlitzky, J. Chan, A.P. McMahon, C.D. Stiles, D.H. Rowitch, Sonic hedgehog-regulated oligodendrocyte lineage genes encoding bHLH proteins in the mammalian central nervous system, *Neuron* 25 (2000) 317–329, [https://doi.org/10.1016/s0896-6273\(00\)80897-1](https://doi.org/10.1016/s0896-6273(00)80897-1).
- [43] B.G. Novitsch, A.I. Chen, T.M. Jessell, Coordinate regulation of motor neuron subtype identity and pan-neuronal properties by the bHLH repressor Olig2, *Neuron* 31 (2001) 773–789, [https://doi.org/10.1016/s0896-6273\(01\)00407-x](https://doi.org/10.1016/s0896-6273(01)00407-x).
- [44] H. Takebayashi, S. Yoshida, M. Sugimori, H. Kosako, R. Kominami, M. Nakafuku, Y. Nabeshima, Dynamic expression of basic helix-loop-helix Olig family members: implication of Olig2 in neuron and oligodendrocyte differentiation and identification of a new member, Olig3, *Mech. Dev.* 99 (2000) 143–148, [https://doi.org/10.1016/s0925-4773\(00\)00466-4](https://doi.org/10.1016/s0925-4773(00)00466-4).
- [45] H. Takebayashi, Y. Nabeshima, S. Yoshida, O. Chisaka, K. Ikenaka, Y. Nabeshima, The basic helix-loop-helix factor olig2 is essential for the development of motoneuron and oligodendrocyte lineages, *Curr. Biol.* 12 (2002) 1157–1163, [https://doi.org/10.1016/s0960-9822\(02\)00926-0](https://doi.org/10.1016/s0960-9822(02)00926-0).
- [46] T.W. Wang, G.P. Stromberg, J.T. Whitney, N.W. Brower, M.W. Klymkowsky, J.M. Parent, Sox3 expression identifies neural progenitors in persistent neonatal and adult mouse forebrain germinative zones, *J. Comp. Neurol.* 497 (2006) 88–100, <https://doi.org/10.1002/cne.20984>.
- [47] Q. Zhou, D.J. Anderson, The bHLH transcription factors OLIG2 and OLIG1 couple neuronal and glial subtype specification, *Cell* 109 (2002) 61–73, [https://doi.org/10.1016/s0092-8674\(02\)00677-3](https://doi.org/10.1016/s0092-8674(02)00677-3).
- [48] K. Lai, B.K. Kaspar, F.H. Gage, D.V. Schaffer, Sonic hedgehog regulates adult neural progenitor proliferation in vitro and in vivo, *Nat. Neurosci.* 6 (1) (2003) 21–27, <https://doi.org/10.1038/nn983>.
- [49] A.M. Falcao, J.A. Palha, A.C. Ferreira, F. Marques, N. Sousa, J. Sousa, Topographical analysis of the subependymal zone neurogenic niche, *PLoS One* 7 (6) (2012) e38647, <https://doi.org/10.1371/journal.pone.0038647>.
- [50] S. Yamamoto, M. Nagao, M. Sugimori, H. Kosako, H. Nakatomi, N. Yamamoto, H. Takebayashi, Y. Nabeshima, T. Kitamura, G. Weinmaster, K. Nakamura, M. Nakafuku, Transcription factor expression and Notch-dependent regulation of neural progenitors in the adult rat spinal cord, *J. Neurosci.* 21 (2001) 9814–9823, <https://doi.org/10.1523/JNEUROSCI.21-24-09814.2001>.
- [51] P. Ellis, B.M. Fagan, S.T. Magness, S. Hutton, O. Taranova, S. Hayashi, A. McMahon, M. Rao, L. Pevny, Sox2, a persistent marker for multipotential neural stem cells derived from embryonic stem cells, the embryo or the adult, *Dev. Neurosci.* 26 (2004) 148–165, <https://doi.org/10.1159/000082134>.
- [52] N. Heins, P. Malatesta, F. Ceconi, M. Nakafuku, K.L. Tucker, M.A. Hack, P. Chapouton, Y.A. Barde, M. Gotz, Glial cells generate neurons: the role of the transcription factor Pax6, *Nat. Neurosci.* 5 (2002) 308–315, <https://doi.org/10.1038/nn828>.
- [53] R. Scardigli, N. Baumer, P. Gruss, F. Guillemot, I. Le Roux, Direct and concentration-dependent regulation of the proneural gene Neurogenin2 by Pax6, *Development* 130 (2003) 3269–3281, <https://doi.org/10.1242/dev.00539>.
- [54] C. Alfaro-Cervello, M. Soriano-Navarro, Z. Mirzadeh, A. Alvarez-Buylla, J.M. Garcia-Verdugo, Biciliated ependymal cell proliferation contributes to spinal cord growth, *J. Comp. Neurol.* 520 (2012) 3528–3552, <https://doi.org/10.1002/cne.23104>.
- [55] E. Furube, H. Ishii, Y. Nambu, E. Kurganov, S. Nagaoka, M. Morita, S. Miyata, Neural stem cell phenotype of tanycyte-like ependymal cells in the circumventricular organs and central canal of adult mouse brain, *Sci. Rep.* 10 (2020) 2826, <https://doi.org/10.1038/s41598-020-59629-5>.